*INTERMATHS, VOL. 5, NO. 2 (**2024**),* **17–33**
https://doi.org/10.22481/intermaths.v5i2.15503

Mathematical Modeling of the Influence of Quarantine Measures and Public Enlightenment on the Transmission Dynamic of Lyme Disease

Imoukhedeme Paul Kehinde [a,*] **and Noah Ismail Aremu** [a]

[a] Department of Mathematics, Usmanu Danfodiyo University, Sokoto, Nigeria

* Correspondence: pimoukhedeme@helpmaninstitute.com

Abstract: In this work, a mathematical model of Lyme disease transmission dynamics with two interacting host populations; humans and rodents were formulated. The quarantine class and public enlightenment campaign parameter are incorporated into human population as means of controlling the spread of the disease. The existence of Disease-Free Equilibrium is investigated. Also, the basic reproduction number were obtained and used for the analysis. The findings revealed that the system is stable when $R_{oh<1}$ and $R_{or} < 1$.From stability analysis, we observed that public enlightenment campaign and isolation of infected people from susceptible people will go a long way to reduce the spread of Lyme disease in the population.

Keywords: Lyme disease; Mathematical Modeling; Transmission Dynamics; Quarantine Measures; Public Enlightenment Epidemiology.

Classification MSC: Primary 92-10; Secondary 92B05.

1 Introduction

Lyme disease is acknowledged as one of the most prevalent tick-borne disease infections in Connecticut, North America. Levi et al. (2012) for which approximately 3,000 cases are reported annually to the Centers for Disease Control and Prevention (CDC,2022). Yet data scientists claim that 300,000 may be more accurate, Kuehn (2013). Recently, the (CDC) estimated that there are approximately 10 times more people diagnosed with Lyme disease than the yearly reported number. Connecticut was the first to experience the uncommon arthritic symptoms. By 1977, the first 51 cases of Lyme arthritis were described, and the Ixodess capularis (black-legged) tick was linked to the transmission of the disease. During 1982, Borrelia burgdorferi, the bacterium that causes Lyme disease, was discovered and the first brochure addressing Lyme disease was developed by the Arthritis Foundation. Serology testing became widely available in Connecticut during 1984. In 1987, Lyme disease became a reportable disease. All physicians were required to report any and all cases of the disease. By 1988, the news of Lyme disease spread and national media attention began. The first federal funding for Lyme disease surveillance, education, and research became available in 1991. Initially, studies and surveys were

Submitted 27 October 2024; Accepted 23 December 2024; Available online: 31 December 2024.
ISSN 2675-8318

conducted to determine the occurrence of the disease in Connecticut and factors that favor acquiring the disease. This work was done by the Connecticut Department of Public Health in collaboration with the Connecticut Agricultural Experiment Station, the University of Connecticut, Yale University, local health departments, and the federal Centers for Disease Control and Prevention. The current focus of the Program is on prevention. The emergence of Lyme disease in Connecticut is attributed in large part to changes in land use. That is, land at one time used for farming has become reforested and increasingly developed for suburban residential use. These changes favor expansion of habitat that supports ticks and wildlife and therefore transmission of tick-borne diseases from animals to people in residential areas and among those who work or recreate outdoors. This research is motivated by the rising number of Lyme disease cases in Canada [1] and the absence of a vaccine, which has become a critical issue for infectious disease specialists. Prevention currently relies on personal protection and environmental measures to avoid tick bites. Hence, this study proposes a mathematical model to explore the transmission dynamics of Lyme disease.

2 Transmission Dynamics of Lyme Disease

The Lyme disease bacteria causing human infection in North America, Borrelia burgdorferi and, rarely, B. mayonii, are spread to people through the bites of infected ticks. Borrelia burgdorferi is spread primarily by the blacklegged tick (or deer tick, lxodess capularis) in the northeastern, mid-Atlantic, and north-central United States, and by the western blackleggedtick (l. pacificus) in the Pacific Coast states. Borrelia mayonii is rarely found in ticks and has only been detected in blacklegged ticks in the north-central United States. Blacklegged ticks have a two-to-three-year life cycle. During this time, they go through four life stages: egg, larva, nymph, and adult. After the egg hatches, the larva and nymph each must take a blood meal to develop to the next life stage, and the female needs blood to produce eggs. Larval and nymphal ticks can become infected with Lyme disease bacteria when feeding on an infected wildlife host, usually a rodent. The bacteria are passed along to the next life stage. Nymphs or adult females can then spread the bacteria during their next blood meal. Female ticks infected with Lyme disease bacteria do not pass them to their offspring. Deer are important sources of blood for ticks and are important to tick survival and movement to new areas. However, deer are not infected with Lyme disease bacteria and do not infect ticks. In most cases, a tick must be attached for 36 to 48 hours or more before the Lyme disease bacterium can be transmitted. If you remove a tick quickly (within 24 hours), you can greatly reduce your chances of getting Lyme disease. However, Lyme disease is said to spread from human to human if not treated for a long time which affects the fetus of an infected pregnant woman. CDC (2021). Typical symptoms include fever, headache, fatigue, and a characteristic skin rash called erythema migrants. If left untreated, it can spread to joints, the heart, and the nervous system. Lyme disease is diagnosed based on symptoms, physical findings (e.g., rash), and the possibility of exposure to infected ticks. Many people with early-stage Lyme disease develop circular rash at the site of the tick bite, usually around to 30 days after being bitten. The untreated case of Lyme disease can result in serious joint pain and or neurological problems and chronic Lyme disease can become deteriorating causing a tremendous decease in quality of life. Therefore, this

research intends to develop a mathematical model of Lyme disease to investigate the transmission dynamics of the disease to control and reduce the spread of the disease.

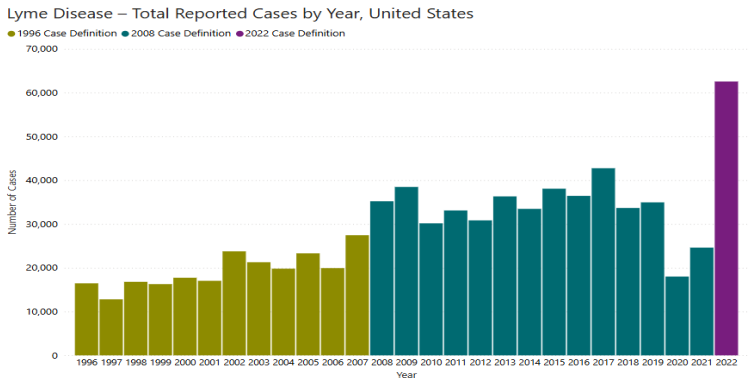

Fig. 1. Lyme disease cases are reported to CDC,USA

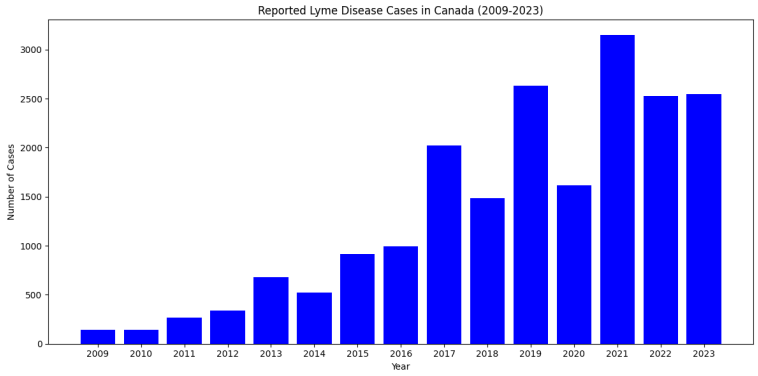

Fig. 2. Lyme disease cases in Canada [2]

3 STATEMENT OF THE PROBLEM

Several mathematical models have been developed by many researchers on transmission dynamics of Lyme disease; [3], [4], [5] and [6] focused on ecological dynamics, climate factors, host population and vector borne (ticks) population in their models.[3]consider quarantine class in their model. In addition,[3], [7], and [5] explicitly consider seasonality of ticks in their models. [3] indirectly addresses seasonality of ticks through the focusing on temperature effects while [4] proposed a model which majorly targeted the development cycle of ticks while [6] examine biotic effects and risk human disease utilizing the ticks' stage structure. In spite of their efforts and preventive measures against the disease; it was discovered that their models could not capture public enlightenment which is very important in tackling transmission of Lyme disease thus, this work proposed to develop a model of Lyme disease incorporating public enlightenment and quarantine.

4 AIM AND OBJECTIVES OF THE STUDY

This research aims at developing a mathematical model of Lyme disease and incorporating public enlightenment and quarantine. This will be achieved through the following objectives to:

1. Develop a mathematical model for the impact of quarantine and public enlightenment on Lyme disease.
2. Investigate the existence and uniqueness of the model.
3. Evaluate the effect of reproduction number (Ro) of the model.
4. Carry out stability analysis of the equilibrium states of the model.
5. Carry out a numerical simulation of the model.

5 SCOPE AND LIMITATION

This study focuses on using mathematical modeling to understand the spread of the disease. The scope includes developing a model, analyzing initial conditions impact, and evaluating intervention strategies. However, the model limitations arise from uncertainties in real-world implementation. Factors such as variations in public compliance and regional differences in disease dynamics could also pose challenges. The study is not accountable for unforeseen variables or external factors influencing the effectiveness of quarantine and awareness strategies.

6 SIGNIFICANCE OF THE STUDY

This study is significant as it explores strategies to control and understand the spread of the disease. Mathematical models help simulate scenarios, offering insights into how interventions like quarantine and public awareness can influence the transmission dynamics, aiding in the development of effective disease management.

7 LITERATURE REVIEW

In a proposed time-delayed Lyme disease model, [5] incorporate some climatic factors in which they obtain the existence of a disease-free periodic solution, introduce the basic reproduction ratio R_0 and show that under the same set of conditions, R_0 serves as a threshold parameter in determining the global dynamics of the model; that is, the disease-free periodic solution is globally attractive if $R_0 < 1$; the system is uniformly persistent and admits a positive periodic solution if $R_0 > 1$. Numerically, they studied the Lyme disease transmission in Long Point, Ontario, Canada. Our simulation results indicate that Lyme disease is endemic in this region if no further intervention is taken. They find out that Lyme disease will die out in this area if they decrease the recruitment rate of larvae, which implies that the disease can be controlled by preventing tick eggs from hatching into larvae. The models developed revealed the

dilution effects of the host population and also in seasonal variations in temperature, humidity, and resource availability have a strong effect on tick population dynamics. Climate impacts tick survival mostly during nonparasitic periods of the life cycle: outside certain ranges of temperature and rainfall, tick populations cannot survive, because these conditions directly kill the ticks or inhibit host-seeking activity. Within these limits, temperature may also determine development rates. For the ecological dynamics governing the velocity of the current epidemic's spread of Lyme disease [6] present a reaction-diffusion model. They find out that the equilibrium density of infectious tick nymphs (hence the risk of human disease) can depend on density-independent survival interacting with biotic effects on the tick's stage structure. The local risk of infection reaches a maximum at an intermediate level of adult tick mortality and at an intermediate rate of juvenile tick attacks on mammalian hosts. If the juvenile tick attack rate is low, an increase generates both a greater density of infectious nymphs and an increased spatial velocity. However, if the juvenile attack rate is relatively high, nymph density may decline while the epidemic's velocity still increases. Velocities of simulated two-dimensional epidemics correlate with the model pathogen's basic reproductive number. To better understand various factors determining the disease risk, which not only enrich our understanding on the ecological cycle of disease transmission [4] proposed a growing body of theoretical models but also promote new theoretical developments on model formulation, analysis and simulation. we provide a review about the models and results we have obtained recently on modeling and analyzing Lyme disease transmission, with the purpose to highlight various aspects in the ecological cycle of disease transmission to be incorporated, including the growth of ticks with different stages in the life cycle, the seasonality, host diversity, spatial disease pattern due to host short distance movement and bird migration, co-infection with other tick-borne pathogens and climate change impact. we identified and compared, 10 years after the European inventory, the characteristics of national surveillance systems and policies for Lyme disease (LD) in humans, with additional countries. The outcome of the study has been used to produce predictive and risk assessment tools for animal health and public health outcomes. To investigate whether the model can be used to identify limits for the potential northward spread of Ixodes scapularis in North America [8] developed a process-based dynamic population model of Ixodes scapularis with the main purpose , that may be imposed by effects of temperature on tick survival. Their model incorporates intra-annual, temperature-dependent variations in the development rates of different tick instars and is well validated by the seasonality pattern of different tick instars. This sort of model structure then has been used in a number of mechanistic models of ticks that aim to predict seasons of tick activity and variations in tick abundance in different locations. However, this structure is mathematically intractable and calculation of the effects of climate change-induced increasing temperatures (or of other environmental changes) on the basic reproduction number R_0 is not directly possible. In the model develop for a transmission dynamics model that includes the interactions between the primary vectors involved: black-legged ticks (Ixodes. scapularis), white-footed mice (Peromyscus leucopus), and white-tailed deer (Odocoileus virginianus) [3] model shows that the presence of multiple vectors may have a significant impact

on the dynamics and spread of Lyme disease. Based on our model, we also calculate the basic reproduction number, R_0 , a threshold value that predicts whether a disease exists or dies out. Subsequent extensions of the model consider seasonality of the tick's feeding period and mobility of deer between counties. Our results suggest that a longer tick peak feeding period results in a higher infection prevalence. Moreover, while the deer mobility may not be a primary factor for short-term emergence of Lyme disease epidemics, in the long-run it can significantly contribute to local infectiousness in neighboring counties, which eventually reach the endemic steady state. A theoretical model by [9] they present that illustrates how reductions in small-mammal predators can sharply increase Lyme disease risk. We then show that increases in Lyme disease in the northeastern and midwestern United States over the past three decades are frequently uncorrelated with deer abundance and instead coincide with a range-wide decline of a key small-mammal predator, the red fox, likely due to expansion of coyote populations. Further, across four states we find poor spatial correlation between deer abundance and Lyme disease incidence, but coyote abundance and fox rarity effectively predict the spatial distribution of Lyme disease in New York. These results suggest that changes in predator communities may have cascading impacts that facilitate the emergence of zoonotic diseases, the vast majority of which rely on hosts that occupy low trophic levels. A simple semi-discrete (ticks' feeding is assumed to occur only during the summers of each year) model for tick population dynamics [7] proposed the conditions for existence, uniqueness, and stability of a positive equilibrium are found; the system is then studied numerically using parameter estimates calibrated for the tick Ixodes ricinus and the sensitivity parameters is examined. Then, this model is extended to consider a tick-transmitted infection of one species of hosts, while other hosts are incompetent to the infection. Assuming, for simplicity, that the infection is not affecting the total number either of hosts or ticks, a threshold condition for infection persistence is obtained. The dependence of the equilibrium infection prevalence on parameters is studied numerically; in particular, we considered how infection prevalence depends on host densities. This analysis reveals that a 'dilution effect' occurs both for competent and for incompetent hosts; this means that, besides a lower threshold for host densities for infection to persist, there exists also an upper threshold: if host densities were higher than the upper threshold, the infection would go to extinction. Numerically, it was found that, for realistic parameter values, the upper threshold is not much higher than observed densities. Based on these literature reviewed and work of[3] and [8], we proposed mathematical modeling of the impact of quarantine and public enlightenment on the transmission dynamics of Lyme disease.

8 METHODOLOGY

8.1 Model Formulation

The model considers two populations of humans and rodents. The human population is subdivided into four compartments: Susceptible, Infected, Quarantined, and Recovered. The rodent population is subdivided into two compartments: Susceptible and Infected.

The human population is recruited into the Susceptible compartment at a constant

recruitment rate. The susceptible humans become infected and move to the infected class by contacting the infected rodents or infected humans at the contact rates $a\Omega_1$ and Ω_2 respectively. Infected humans move to the quarantine class at the rate τ, and the quarantined individuals move to the recovered class after treatment at the recovery rate γ_h. Individuals leave the population either by the natural death rate μ_h or by disease-induced death rate δ_h. The parameter β measures the effectiveness of the enlightenment campaign, where $0 \leq \beta \leq 1$, and θ is the effectiveness of quarantine and treatment, where $0 \leq \theta \leq 1$. It is assumed that death due to disease is influenced by the effectiveness of treatment; hence it is given by $(1-\theta)\delta_h$.

The rodent population is recruited into the Susceptible compartment at a constant recruitment rate Λ_r. The susceptible rodents become infected and move to the infected class by contacting infected rodents at the contacting rate Ω_3. The infected rodents leave the population either by the natural death rate μ_r or by disease-induced death rate. We also assume that since the wild rodents may not have access to treatment, they do not recover from the disease.

The schematic diagram is represented in Figure 3.

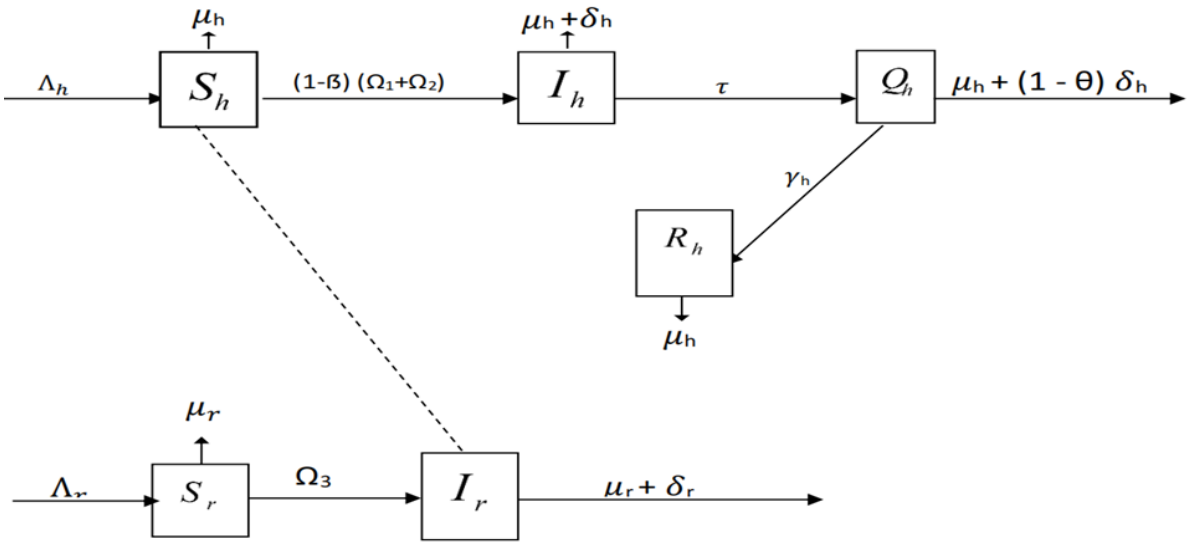

Fig. 3. Schematic diagram of the model.

9 Model Formulation

The model for the dynamics of Lyme disease is given by the subsequent deterministic system of linear differential equations. The model equations are derived as follows:

$$\frac{dS_h}{dt} = \Lambda_h - (1-\beta)\left(\frac{\Omega_1 I_r}{N_h} + \frac{\Omega_2 I_h}{N_h}\right) S_h - \mu_h S_h \tag{9.1}$$

$$\frac{dI_h}{dt} = (1-\beta)\left(\frac{\Omega_1 I_r}{N_h} + \frac{\Omega_2 I_h}{N_h}\right) S_h - (\mu_h + \delta_h + \tau) I_h \tag{9.2}$$

$$\frac{dQ_h}{dt} = \tau I_h - (\mu_h + \gamma_h + (1-\theta)\delta_h)\, Q_h \tag{9.3}$$

$$\frac{dR_h}{dt} = \gamma_h Q_h - \mu_h R_h \tag{9.4}$$

$$\frac{dS_r}{dt} = \Lambda_r - \frac{\Omega_3 I_r S_r}{N_r} - \mu_r S_r \tag{9.5}$$

$$\frac{dI_r}{dt} = \frac{\Omega_3 I_r S_r}{N_r} - (\mu_r + \delta_r) I_r. \tag{9.6}$$

Where $0 \leq \beta \leq 1$ and $0 \leq \theta \leq 1$.
The total populations are defined as:

$$N_h = S_h + I_h + Q_h + R_h, \quad N_r = S_r + I_r$$

$$N = N_h + N_r = S_h + I_h + Q_h + R_h + S_r + I_r$$

So that the total population dynamics can be expressed as:

$$\frac{dN}{dt} = \Lambda - \mu N - (\delta I + (1-\theta) S_h Q_h)$$

$$\frac{dN}{dt} = \Lambda - \mu N.$$

Table 1. Table of Variables and Parameters

NO	Variables/Parameters
1.	Λ_h - Constant recruitment rate of humans
2.	Λ_r - Constant recruitment rate of rodents
3.	S_h - Susceptible humans
4.	I_h - Infected humans
5.	Q_h - Quarantined humans
6.	R_h - Recovered humans
7.	S_r - Susceptible rodents
8.	I_r - Infected rodents
9.	μ_h - Natural death rate of humans
10.	μ_r - Natural death rate of rodents
11.	β - Effectiveness of public enlightenment campaign
12.	θ - Effectiveness of quarantine and treatment
13.	Ω_1 - Contact rate of rodents to humans
14.	Ω_2 - Contact rate of humans to humans
15.	Ω_3 - Contact rate of rodents to rodents
16.	τ - Progression rate from infected to quarantine
17.	δ_h - Disease-induced death rate of humans
18.	δ_r - Disease-induced death rate of rodents
19.	γ_h - Recovery rate of humans

10 Basic Properties of the Model Equations

10.1 Invariant Region

The population size can be determined by the linear differential equation of the model formulated:

$$\frac{dN}{dt} = \frac{dS_h}{dt} + \frac{dI_h}{dt} + \frac{dQ_h}{dt} + \frac{dR_h}{dt} + \frac{dS_r}{dt} + \frac{dI_r}{dt} \tag{10.1}$$

i.e.

$$\frac{dN}{dt} = \Lambda - \mu N - (\delta I + (1-\theta)S_h Q_h) \tag{10.2}$$

Such that

$$\frac{dN}{dt} \leq \Lambda - \mu N \tag{10.3}$$

Since $N = N_h = S_h + I_h + Q_h + R_h + S_r + I_r$ and equations (3.1.1) to (3.1.6) resolve to a linear differential equation of the form:

$$\frac{dN}{dt} + \mu N \leq \Lambda \tag{10.4}$$

Theorem 10.1. *The solution of the system of equations is feasible for $t < 0$ if they are in the invariant region Ω.*

Proof: Let $(S_h, I_h, Q_h, R_h, S_r, I_r) \in \mathbb{R}^6$ be any solution of the system with non-negative initial conditions using the integrating factor:

$$\text{I.F.} = e^{\int p\,dt} = e^{\mu t + c} = e^{\mu t} e^{c} = Ae^{\mu t}$$

Thus,

$$Ae^{\mu t}\frac{dN}{dt} = \int Ae^{\mu t}\Lambda\,dt$$

Integrating both sides gives:

$$\int Ae^{\mu t}\,dN = \int Ae^{\mu t}\Lambda\,dt$$

This leads to:

$$Ae^{\mu t}N = \frac{\Lambda Ae^{\mu t}}{\mu} + c$$

Rearranging yields:

$$N = \frac{\Lambda Ae^{\mu t}}{\mu e^{\mu t}} + \frac{c}{\mu Ae^{\mu t}}$$

Thus,

$$N(t) = \frac{\Lambda}{\mu} + ce^{-\mu t}$$

At $t = 0$, the initial population becomes:

$$N(0) = \frac{\Lambda}{\mu} + c$$

Where c is a constant. Simplifying, we have:

$$c = N_0 - \frac{\Lambda}{\mu}$$

Substituting gives:

$$N(t) = \frac{\Lambda}{\mu} + \left(N_0 - \frac{\Lambda}{\mu}\right) e^{-\mu t}$$

By simplification, we obtain:

$$N(t) = \frac{\Lambda}{\mu}\left(1 - e^{-\mu t}\right) + N_0 e^{-\mu t}$$

And therefore,

$$N(0) \leq \frac{\Lambda}{\mu}$$

As $t \to \infty$ in the human population N approaches:

$$C = \frac{\Lambda}{\mu} \quad \text{i.e.,} \quad N \to C,$$

where C is the carrying capacity. Hence, all feasible solutions of the population model system above enter the region Ω:

$$\Omega = \{(S_h, I_h, Q_h, R_h, S_r, I_r) \in \mathbb{R}^6_+ : S_h + I_h + Q_h + R_h + S_r + I_r \geq 0 \quad \text{and} \quad N \leq \frac{\Lambda}{\mu}\}$$

Thus, it is a positively invariant set under the flow induced by the model, which is epidemiologically well-posed in the domain. Furthermore, the usual existence, continuity, and uniqueness results hold for the system.

11 Existence of Equilibria (E^*)

At any equilibrium state, the rate of change of each variable is equal to zero, i.e.,

$$\frac{dN}{dt} = \frac{dS_h}{dt} = \frac{dI_h}{dt} = \frac{dQ_h}{dt} = \frac{dR_h}{dt} = \frac{dS_r}{dt} = \frac{dI_r}{dt} \tag{11.1}$$

At any equilibrium state, let

$$(S_h, I_h, Q_h, R_h, S_r, I_r) = (S_h^*, I_h^*, Q_h^*, R_h^*, S_r^*, I_r^*)$$

where:

$$A_1 = (1-\beta), \quad A_2 = (\mu_h + \delta_h + \tau), \quad A_3 = (\mu_h + \delta_h + (1-\theta)\gamma_h), \quad A_4 = (\mu_r + \delta_r).$$

Thus, from equations (1) to (6), we have that at any arbitrary state:

$$\Lambda_h - (1-\beta)\left(\frac{\Omega_1 I_r^*}{N_h} + \frac{\Omega_2 I_h^*}{N_h}\right) S_h^* - \mu_h S_h^* = 0 \tag{11.2}$$

$$(1-\beta)\left(\frac{\Omega_1 I_r^*}{N_h} + \frac{\Omega_2 I_h^*}{N_h}\right) S_h^* - (\mu_h + \delta_h + \tau) I_h^* = 0 \tag{11.3}$$

$$\tau I_h^* - (\mu_h + \gamma_h + (1-\theta)\delta_h) Q_h^* = 0 \tag{11.4}$$

$$dRhdt = \gamma_h Q_h - \mu h Rh \gamma_h Q_h^* - \mu_h R_h^* = 0 \tag{11.5}$$

$$\Lambda_r - \frac{\Omega_3 I_r^* S_r^*}{N_r} - \mu_r S_r^* = 0 \tag{3.3.7}$$

$$\frac{\Omega_3 I_r^* S_r^*}{N_r} - (\mu_r + \delta_r) I_r^* = 0 \tag{11.6}$$

Hence, we conclude that $I_h^* = I_r^* = 0$.

12 Disease-Free Equilibrium (E^0)

At disease-free equilibrium, there is an absence of disease. Thus, the disease-free equilibrium E^0 for the model is given as:

$$I_h^* = Q_h^* = R_h^* = 0$$

By solving the model equations using the idea of [11], we have:
Let

$$(S_h^*, I_h^*, Q_h^*, R_h^*, S_r^*, I_r^*) = (S_h^0, I_h^0, Q_h^0, R_h^0, S_r^0, I_r^0) = E^0$$

Thus,

$$E^0 = (S_h^0, I_h^0, Q_h^0, R_h^0, S_r^0, I_r^0) = \left(\frac{\Lambda}{\mu}, 0, 0, 0, \frac{\Lambda}{\mu}, 0\right)$$

At disease-free equilibrium, we have:

$$N_h^0 = \frac{\Lambda_h}{\mu_h} \quad \text{and} \quad N_r^0 = \frac{\Lambda_r}{\mu_r}$$

12.1 Basic Reproduction Number R_0

The basic reproduction number R_0 is a crucial concept in epidemiology that quantifies the average number of secondary infections produced by a single infected individual in a population where everyone is susceptible. It is a key parameter in infectious disease modeling and is used to assess the potential for an outbreak to become an epidemic.

Using the next generation matrix approach as described in [10] and [11], the basic reproduction number is defined as the highest eigenvalue of the matrix FV^{-1}, where F represents the transmission terms and V represents the transition terms in the model.

The matrices F and V are defined as follows:

$$F = \begin{bmatrix} A_1\Omega_2 & A_1\Omega_1 \\ 0 & \Omega_4 \end{bmatrix}, \quad V = \begin{bmatrix} A_2 & 0 \\ 0 & A_4 \end{bmatrix}, \quad V^{-1} = \begin{bmatrix} \frac{1}{A_2} & 0 \\ 0 & \frac{1}{A_4} \end{bmatrix}$$

Calculating FV^{-1}:

$$FV^{-1} = \begin{bmatrix} \frac{A_1\Omega_2}{A_2} & \frac{A_1\Omega_1}{A_4} \\ 0 & \frac{\Omega_3}{A_4} \end{bmatrix}$$

There exist two reproduction numbers since the transformation is between rodents and humans. Hence,

$$R_{0h} = \frac{A_1\Omega_2}{A_2}$$

which is the basic reproduction number from humans to humans, and

$$R_{0r} = \frac{\Omega_3}{A_4}$$

which is the basic reproduction number from rodents to rodents.

12.2 Local Stability of Disease-Free Equilibrium

The linear stability can be established using the next generation operator method on the system developed by [12]. Using the notation by [13] , the matrices F and V, for the new infection and the remaining transmission terms, are respectively given by the disease-free equilibrium of the model system . The equilibrium is locally asymptotically stable if $R_{0h} < 1$ or $R_{0r} < 1$.

Proof using Jacobian stability techniques, as in [14]. The Jacobian matrix is given as:

$$J(E^0) = \begin{vmatrix} -\mu_h & -A_1\Omega_2 & 0 & 0 & 0 & -A_1\Omega_2 \\ 0 & -A_1\Omega_2 - A_1 & 0 & 0 & 0 & -A_1\Omega_1 \\ 0 & \tau & -A_2 & 0 & 0 & 0 \\ 0 & 0 & \Upsilon_h & -\Upsilon_h & 0 & 0 \\ 0 & 0 & 0 & 0 & -\mu_r & -\Omega_2 \\ 0 & 0 & 0 & 0 & 0 & A_1 \end{vmatrix}$$

12.3 Jacobian Matrix and Stability Analysis

Reducing to an upper triangular matrix gives:

$$J(E^0) = \begin{vmatrix} -\mu_h & -A_1\Omega_1 & 0 & 0 & 0 & -A_1\Omega_1 \\ 0 & A_1\Omega_2 & 0 & 0 & 0 & A_1\Omega_1 \\ 0 & 0 & -A_3 & 0 & 0 & \frac{-A_1\Omega_1\tau}{A_1\Omega_2 - A_2} \\ 0 & 0 & 0 & -\mu_h & 0 & \frac{-A_1\Omega_1\Upsilon_h\tau}{A_3(A_1\Omega_2 - A_2)} \\ 0 & 0 & 0 & 0 & -\mu_r & -\Omega_3 \\ 0 & 0 & 0 & 0 & 0 & \Omega_3 - A_4 \end{vmatrix}$$

The characteristic equation is given by:

$$|J(E^0) - \lambda I| = 0$$

$$\left| \begin{vmatrix} -\mu_h - \lambda & -A_1\Omega_1 & 0 & 0 & 0 & -A_1\Omega_1 \\ 0 & A_1\Omega_2 - A_2 - \lambda & 0 & 0 & 0 & A_1\Omega_1 \\ 0 & 0 & -A_3 - \lambda & 0 & 0 & \frac{-A_1\Omega_1\tau}{A_1\Omega_2 - A_2} \\ 0 & 0 & 0 & -\mu_h - \lambda & 0 & \frac{-A_1\Omega_1\Upsilon_h\tau}{A_3(A_1\Omega_2 - A_2)} \\ 0 & 0 & 0 & 0 & -\mu_r - \lambda & -\Omega_3 \\ 0 & 0 & 0 & 0 & 0 & \Omega_3 - A_4 - \lambda \end{vmatrix} \right| = 0$$

The characteristic equation is given as:

$$(\mu_h - \lambda)(A_1\Omega_2 - A_2 - \lambda)(-A_3 - \lambda)(-\mu_r - \lambda)(-\mu_h - \lambda)(\Omega_3 - A_4 - \lambda) = 0$$

The eigenvalues are:

$$\lambda_1 = -\mu, \quad \lambda_2 = A_1\Omega_2 - A_2, \quad \lambda_3 = -A_3, \quad \lambda_4 = -\mu_h, \quad \lambda_5 = -\mu_r, \quad \lambda_6 = \Omega_3 - A_4$$

It is observed from the equations that all the eigenvalues λ are less than zero except λ_2 and λ_6.

For $\lambda_2 < 0$:

$$A_1\Omega_2 - A_2 < 0 \implies \frac{A_1\Omega_2}{A_2} < 1$$

This implies:

$$R_{0h} < 1$$

For $\lambda_6 < 0$:

$$\Omega_3 - A_4 < 0 \implies \frac{\Omega_3}{A_4} < 1$$

This implies:

$$R_{0r} < 1$$

Hence, the disease-free equilibrium (DEF) is locally asymptotically stable. This proves that the disease will not persist in the population.

13 Sensitivity analysis and Numerical Simulation

Sensitivity analysis is a crucial analysis that shows the importance of each parameter to Lyme disease transmission. A graphical simulation was formulated using maple software showing the effectiveness of the enlightenment Campaign β which predicts the reproduction number R_0 of the disease.

Parameter	Value	Parameter	Value
A_h	0.029	μ_h	1.5
A_r	0.2	δ_h	0.2
Ω_1	0.00025	Y_h	0.83
Ω_2	0.00006	τ	0.52
Ω_3	0.027	β	0.005
μ_r	0.002	θ	0.005
δ_r	0.5	N_h	164700000
		N_r	150000000

Fig. 4. Parameters and Values

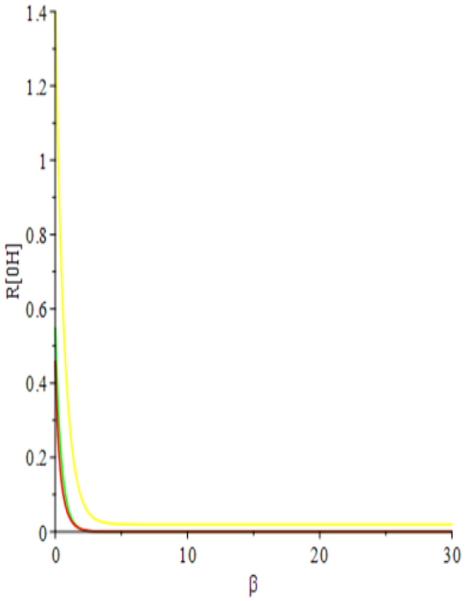

Fig. 5. Schematic diagram of the model.

Figure 4 & 5 shows simulation of basic reproduction number of humans against public enlightenment campaign at lower effective rate. The graph illustrates the relationship between the basic reproduction number of humans, denoted as R_{0h}, and the public enlightenment campaign, represented by β, at a contact rate Ω_2. It shows that as the effectiveness of the enlightenment campaign β increases, the basic reproduction number R_{0h} decreases. Conversely, it was observed that the lower the effectiveness of the campaign, the higher the reproduction number R_0.

The figure 6 & 7 illustrates the relationship between the basic reproduction number of humans, denoted as R_{0h}, and the public enlightenment campaign, represented by β, at a contact rate Ω_2. It shows that as the effectiveness of the enlightenment campaign β increases, the basic reproduction number R_{0h} decreases. This indicates that a higher effectiveness of the campaign correlates with a lower reproduction number.

Parameter	Value	Parameter	Value
A_h	0.029	μ_h	1.5
A_r	0.2	δ_h	0.2
Ω_1	0.00025	Y_h	0.83
Ω_2	0.00006	τ	0.52
Ω_3	0.027	β	2.6
μ_r	0.002	θ	2.4
δ_r	0.5	N_h	164700000
		N_r	150000000

Fig. 6. Parameters and Values

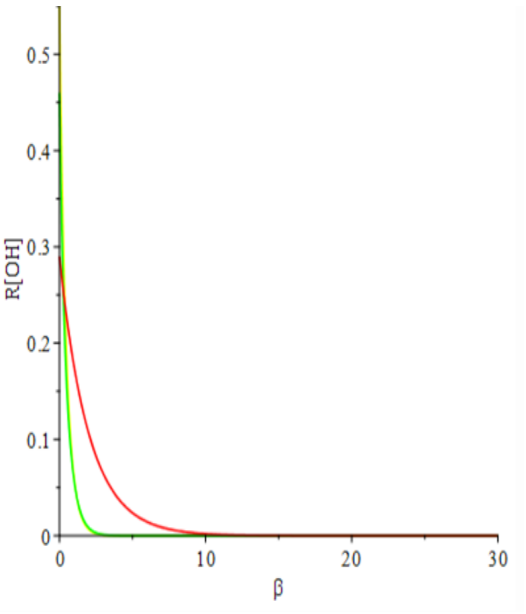

Fig. 7. Schematic diagram of the model.

Parameter	Value	Parameter	Value
A_h	0.029	μ_h	1.5
A_r	0.2	δ_h	0.2
Ω_1	0.00025	Y_h	0.83
Ω_2	0.00006	τ	0.52
Ω_3	0.027	β	0.5
μ_r	0.002	θ	0.5
δ_r	0.5	N_h	164700000
		N_r	150000000

Fig. 8. Parameters and Values

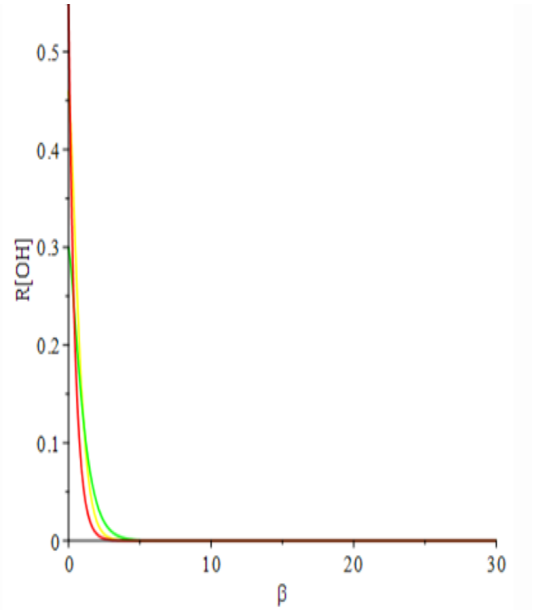

Fig. 9. Schematic diagram of the model.

Figure 8 & 9 illustrates the simulation of the basic reproduction number of humans, denoted as R_{0h}, in relation to the public enlightenment campaign, represented by β, at a contact rate Ω_2. The graph demonstrates that as the effectiveness of the enlightenment campaign β increases, the basic reproduction number R_{0h} decreases. This trend indicates that a more effective campaign correlates with a lower reproduction number.

Furthermore, the results reveal that a higher public enlightenment campaign, coupled with an increased progression rate from infected individuals to quarantine, leads to a further reduction in the basic reproduction number. This finding implies that public

enlightenment campaigns, along with the isolation of infected individuals from susceptible populations, are crucial strategies in mitigating the spread of Lyme disease within the affected population.

14 Conclusion

The Lyme disease transmission dynamics model incorporating quarantine class and public enlightenment campaign parameter to control the spread of the disease was developed using first order ordinary differential equations. Two equilibrium states exist in the model; Disease Free Equilibrium (DFE) and Endemic Equilibrium (EE). There are also two reproduction numbers in the model; rodent to human transmission reproduction number and human to human reproduction number. The local and global stability of DFE is stable which implies that the disease will not persist in the population. furthermore, the graphical simulation of basic reproduction number and some parameters of the model are show in order to understand the effect of these parameters in the spread and control of Lyme. Hence the result can further be extended by incorporating additional variables and parameters. [9],[14–16].

Conflicts of Interest: The authors declare no conflict of interest in the writing of the manuscript, or in the decision to publish the results.

ORCID

O. Adedire https://orcid.org/0000-0003-3790-7776
P.C. Mordi https://orcid.org/0009-0006-3265-4449

References

1. G News, Lyme disease vaccine: What happened to the lymerix vaccine? (2024) Accessed: 2024-10-26.
2. K Murison, et al., Epidemiology and clinical manifestations of reported lyme disease cases: Data from the canadian lyme disease enhanced surveillance system. *PLoS ONE* **18**, e0295909 (2023) Accessed: 2024-10-26.
3. A Nguyen, J Mahaffy, NK Vaidya, Modeling transmission dynamics of lyme disease: Multiple vectors, seasonality, and vector mobility. *Infect. Dis. Model.* **4**, 28–43 (2019).
4. L Yijun, W Jianhog, Modelling lyme disease transmission. *Chin. Med. J.* **2**, 229–243 (2017).
5. X Wang, XQ Zhao, Dynamics of a time-delayed lyme disease model with seasonality. *SIAM J. on Appl. Dyn. Syst.* **16**, 853–889 (2017).
6. T Caraco, et al., Stage-structured infection transmission and a spatial epidemic: a model for lyme disease. *The Am. Nat.* **160**, 348–359 (2002).
7. M Ghosh, A Pugliese, Seasonal population dynamics of ticks, and its influence on infection transmission: a semi-discrete approach. *Bull. Math. Biol.* **66**, 1659–1684 (2004).
8. CL Ogden, MD Carroll, KM Flegal, Prevalence of overweight and obesity in the united states, 1999-2004. *JAMA* **295**, 1549–1555 (2005).
9. T Levi, AM Kilpatrick, M Mangel, CC Wilmers, Deer, predators, and the emergence of lyme disease. *Proc. Natl. Acad. Sci.* **109**, 10942–10947 (2012).
10. O Diekmann, JAP Heesterbeek, JAJ Metz, On the definition and the computation of the basic reproduction ratio r in models for infectious diseases in heterogeneous populations. *J. Math. Biol.* **28**, 365–382 (1990).

11. P Driessche Van Den, J Watmough, Reproduction numbers and subthreshold endemic equilibria for compartmental models of disease transmission. *Math. Biosci.* **180**, 29–48 (2002).
12. O Diekmann, JA Heesterbeek, MG Roberts, Construction of next-generation matrices for compartmental epidemic models. *Model. Build. Comput. Biol.* **26**, 360–381 (2000).
13. MY Chong, JA Smith, R Doe, Title of the study. *J. Name* **Volume**, Page range (2023).
14. P Van den Driessche, J Watmough, Reproduction numbers and sub-threshold endemic equilibria for compartmental models of disease transmission. *Math. Biosci.* **180**, 29–48 (2002).
15. BM Kuehn, Cdc estimates 300,000 us cases of lyme disease annually. *JAMA* **310**, 1110–1110 (2013).
16. Centers for Disease Control and Prevention, Lyme disease (2021) Retrieved from https://www.cdc.gov/lyme/index.html.